MATERIAIS INTELIGENTES
PARA A RADIOCIÊNCIA

17º
CONGRESSO DO COMITÉ
PORTUGUÊS DA URSI

Electromagnetic Solution of Large and Deep-multiscale Problems using Surface Integral Equation Techniques

Víctor F. Martín(1), Diego M. Solís(1), José L. Rodríguez(2), Fernando Obelleiro(2), Luis Landesa(1), and **<u>Jose M. Taboada</u>**(1)

[1] Dept. Tecnología de Computadores y Comunicaciones, **University of Extremadura**, Spain
[2] Dept. Teoría de la Señal y Comunicaciones, **University of Vigo**, Spain

Where we are...

Ferrol
A Coruña
Santiago de Compostela
Lugo
Vigo
Ourense
Gijón
Avilés
Oviedo
Llanes
Santander
Bilbao
San Sebastián
Bayona
Pau
Lourdes
Toulouse
Albi
Montpellier
Nimes
Béziers
Carcasona
Narbona
Perpiñán
Andorra
Vitoria-Gasteiz
Pamplona
Logroño
Burgos
León
Ponferrada
Benavente
Palencia
Braganza
Valladolid
Zamora
Braga
Guimarães
Oporto
Vila Real
Salamanca
Ávila
Aveiro
Viseu
Coimbra
Figueira da Foz
Portugal
Plasencia
Cáceres
Madrid
Alcalá de Henares
Getafe
Toledo
Cuenca
Teruel
Huesca
Zaragoza
Lérida
Girona
Lloret de Mar
Barcelona
Tarragona
Castellón de la Plana
Valencia
España
Mar Balear
Alcudia
Palma
Santa Ponsa
Manacor
Maó-Mahón
Ibiza
Caldas da Rainha
Lisboa
Évora
Mérida
Badajoz
Ciudad Real
Albacete
Gandia
Denia
Calpe
Alicante (Alacant)
Benidorm
Murcia
Lorca
Cartagena
Linares
Córdoba
Jaén
Úbeda
Sevilla
Huelva
Granada
Albufeira
Faro
Cádiz
Ronda
Málaga
Marbella
Motril
Almería
Roquetas de Mar
Gibraltar
Argel
Chlef
Blida
Bouira
Oued Rhiou

Motivation and objectives

Solving real-life problems involving complicated assemblies, including multiscale geometrical features and multiple materials.

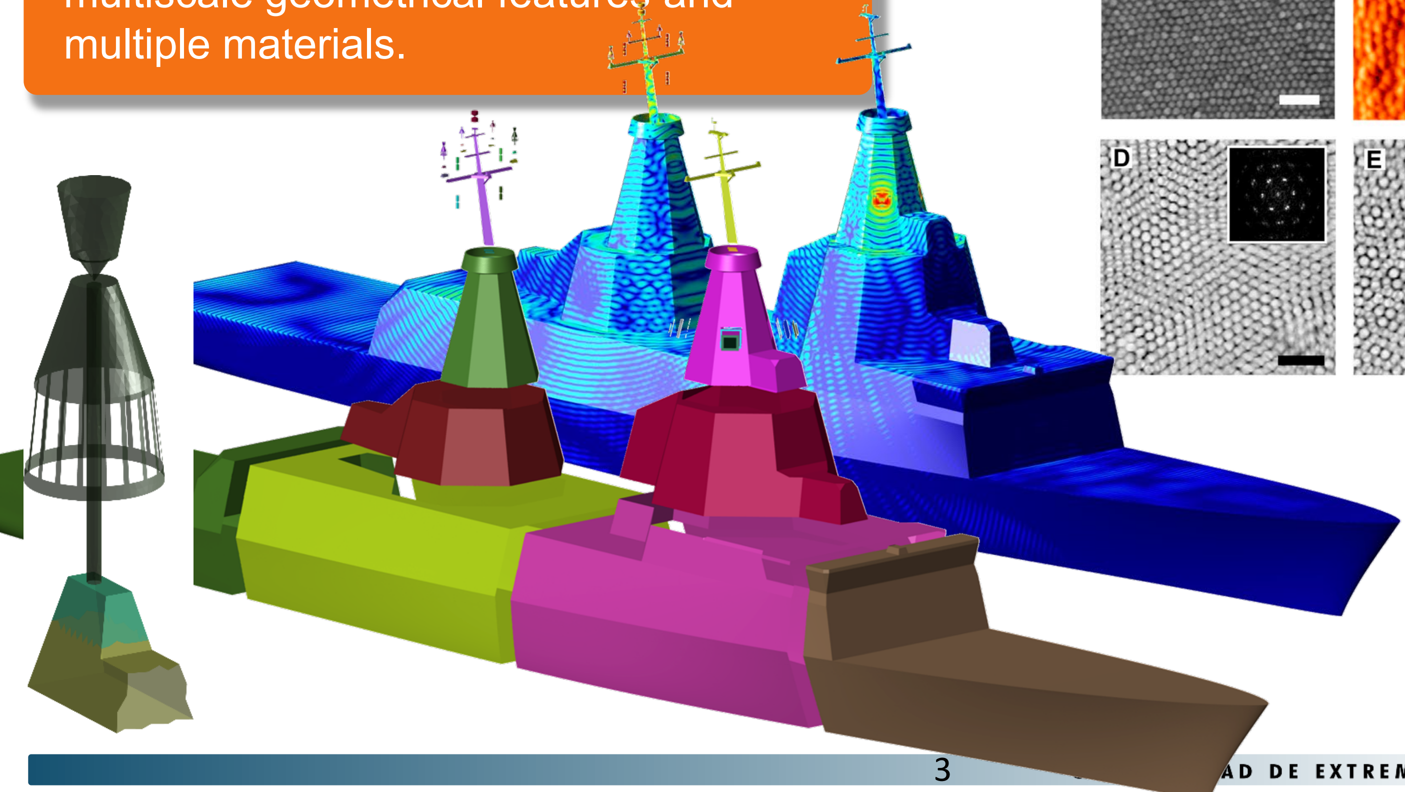

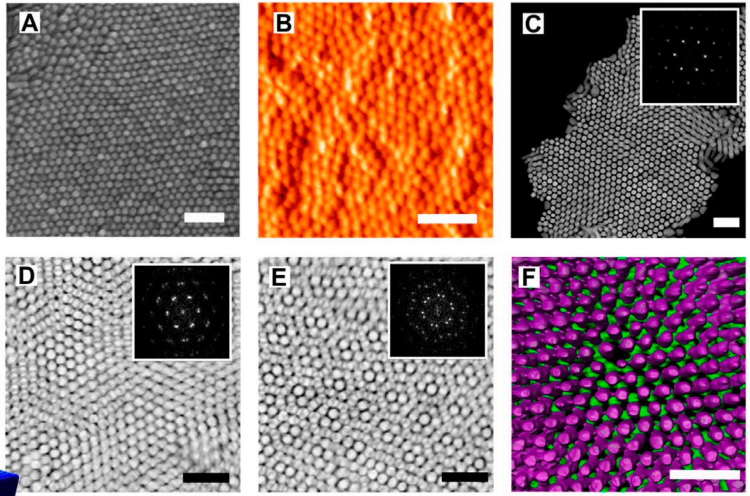

Fast & accurate solution of large multiscale problems

Surface integral equations (SIE)
Method of Moments

Multilevel fast multipole algorithm – fast Fourier transform (MLFMA – FFT)

Highly scalable paralelization

Domain decomposition method (DDM)

Discontinuous Galerkin (DG)

Multiresolution quasi-Helmholtz decomposition

Surface Integral Equations (SIE) based Method of Moments

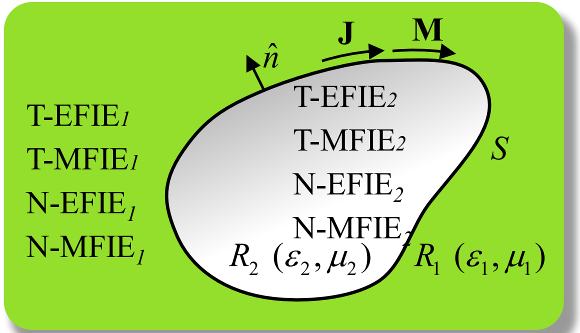

$-\hat{\mathbf{n}}\times\hat{\mathbf{n}}\times \rightarrow$ Tangential (T)-formulations

$\hat{\mathbf{n}}\times \rightarrow$ Twisted or normal (N)-formulations

Stratton-Chu integro-differential operators

$$\mathcal{L}(\mathbf{X}) = jk\int_S \mathbf{X}(\mathbf{r}')G(\mathbf{r},\mathbf{r}')\,ds' - \frac{1}{jk}\nabla\int_S \nabla'\cdot\mathbf{X}(\mathbf{r}')G(\mathbf{r},\mathbf{r}')\,ds'$$

$$\mathcal{K}(\mathbf{X}) = PV\int_S \mathbf{X}(\mathbf{r}')\times\nabla G(\mathbf{r},\mathbf{r}')\,ds'$$

Green's function

$$G(\mathbf{r},\mathbf{r}') = \frac{e^{-jk|\mathbf{r}-\mathbf{r}'|}}{4\pi|\mathbf{r}-\mathbf{r}'|}$$

$$\text{T-EFIE}_l : \left(\eta_l\mathcal{L}_l(\mathbf{J}_l) - \mathcal{K}_l(\mathbf{M}_l)\right)_{\tan} + \frac{1}{2}\hat{\boldsymbol{n}}_l\times\mathbf{M}_l = \left(-\mathbf{E}_l^{\text{inc}}\right)_{\tan}$$

$$\text{T-MFIE}_l : \left(\mathcal{K}_l(\mathbf{J}_l) + \frac{1}{\eta_l}\mathcal{L}_l(\mathbf{M}_l)\right)_{\tan} - \frac{1}{2}\hat{\boldsymbol{n}}_l\times\mathbf{J}_l = \left(-\mathbf{H}_l^{\text{inc}}\right)_{\tan}$$

$$\text{N-EFIE}_l : \hat{\boldsymbol{n}}_l\times\left(\eta_l\mathcal{L}_l(\mathbf{J}_l) - \mathcal{K}_l(\mathbf{M}_l)\right) - \frac{1}{2}\mathbf{M}_l = \hat{\boldsymbol{n}}_l\times\mathbf{E}_l^{\text{inc}}$$

$$\text{N-MFIE}_l : \hat{\boldsymbol{n}}_l\times\left(\mathcal{K}_l(\mathbf{J}_l) + \frac{1}{\eta_l}\mathcal{L}_l(\mathbf{M}_l)\right) + \frac{1}{2}\mathbf{J}_l = \hat{\boldsymbol{n}}_l\times\mathbf{H}_l^{\text{inc}}$$

$$\textbf{JCFIE: } \sum_{l=1}^{2} a_l \frac{1}{\eta_l}\text{T-EFIE}_l + \sum_{l=1}^{2} b_l\,\text{N-MFIE}_l$$

$$\textbf{MCFIE:} -\sum_{l=1}^{2} c_l\,\text{N-EFIE}_l + \sum_{l=1}^{2} d_l\eta_l\,\text{T-MFIE}_l$$

Galerkin Method of moments

Parallel-prone MLFMA-FFT

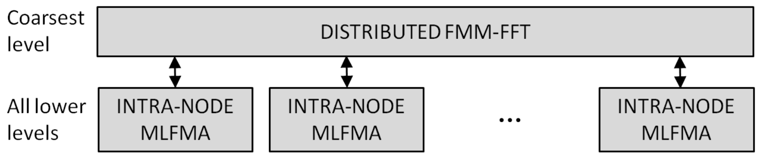

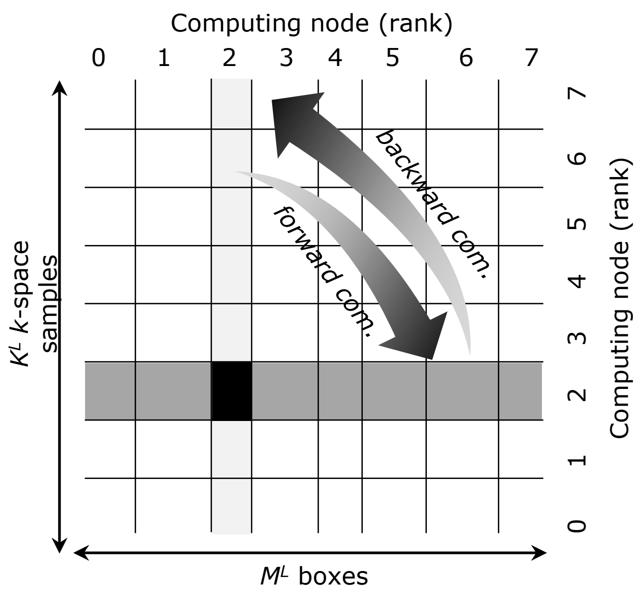

MVP

MLFMA: aggregation, interpolation, near-field translation

Forward communication

FMM-FFT: 3D-FFT far-field translation

Backward communication

MLFMA: anterpolation, disaggregation

Communication of noncontiguous data layout, because of the distributed transposition.

Nonuniform communication volumes, because the size of the actual transferred data to each node differs.

J. M. Taboada, M. G. Araújo, F. Obelleiro, J. L. Rodríguez, L. Landesa, "MLFMA-FFT parallel algorithm for the solution of extremely large problems in electromagnetics," ***Proceedings of the IEEE***, vol. 101, no. 2, pp. 350-363, Feb. 2013.

Highly scalable parallelization

Hybrid parallel programming

- Message passing interface (MPI) for distributed computations (FMM-FFT)
- OpenMP standard for shared-memory computations (MLFMA)
- Optimal scheme for mixed-memory architectures

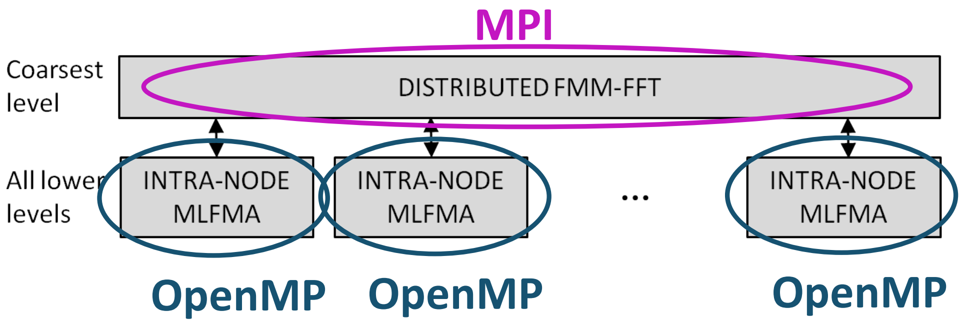

J. M. Taboada, M. G. Araújo, F. Obelleiro, J. L. Rodríguez, L. Landesa, "MLFMA-FFT parallel algorithm for the solution of extremely large problems in electromagnetics," ***Proceedings of the IEEE***, vol. 101, no. 2, pp. 350-363, Feb. 2013.

Domain Decomposition Method (DDM)

- Divide and conquer approach
- Excellent preconditioner for multi-scale problems (isolating different scales in different smaller subdomains)

- 14 subdomains, 121 surfaces & junctions.
- Superstructure subdomains: MLFMA CFIE
- Antenna subdomains: MoM CFIE (ground) / EFIE (patch & patch-ground junctions)

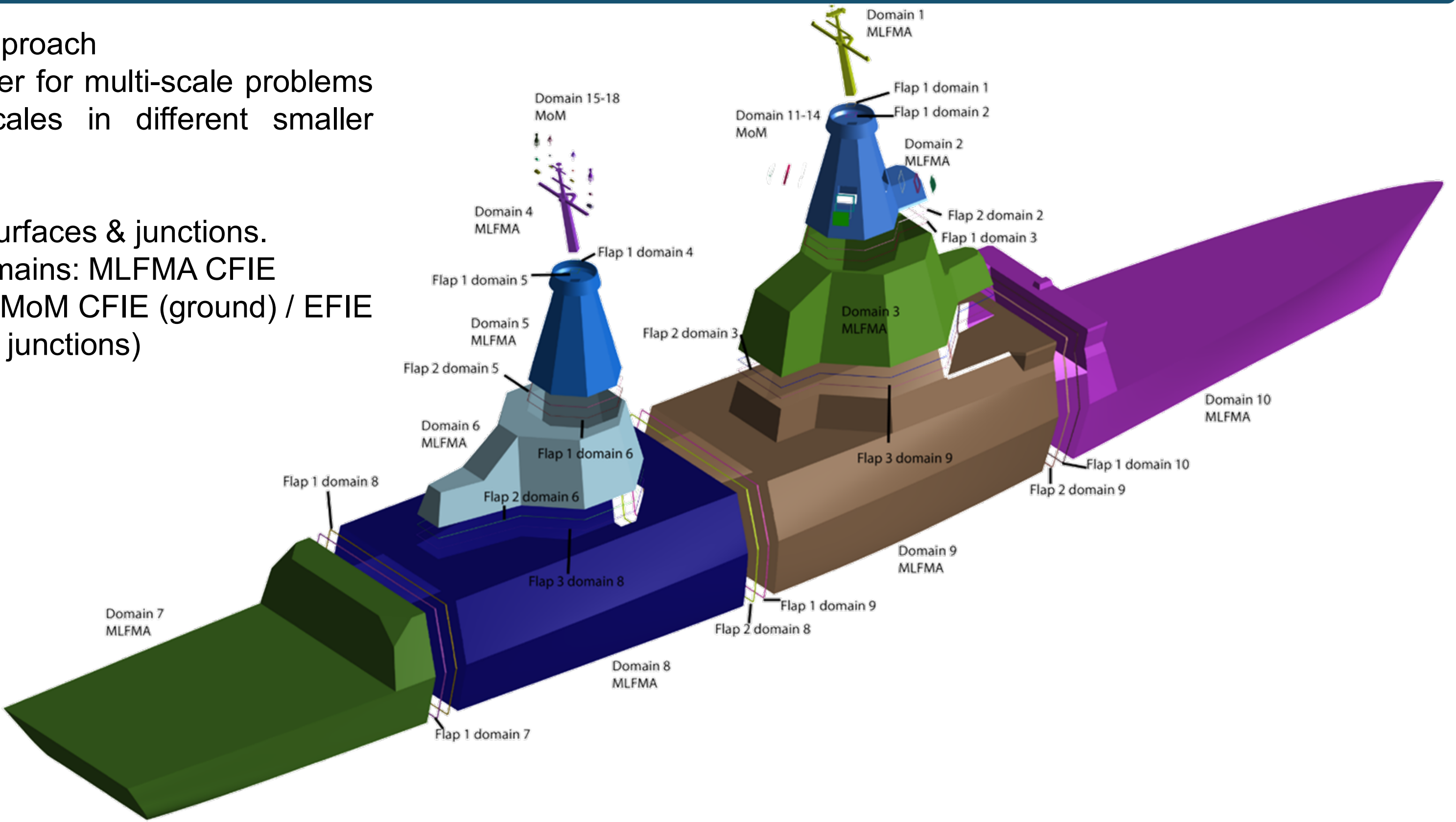

D. M. Solís, V. F. Martín, M. G. Araújo, D. Larios, F. Obelleiro, and J. M. Taboada, "Accurate EMC Engineering on Realistic Platforms Using an Integral Equation Domain Decomposition Approach," ***IEEE Trans. Antennas Propag.***, vol. 68, no.4, pp. 3002 – 3015, Apr. 2020,

Domain Decomposition (DDM)

$$\mathbf{Z} \cdot \boldsymbol{I} = \boldsymbol{V}$$

$$\mathbf{P} \cdot \mathbf{Z} \cdot \boldsymbol{I} = \mathbf{P} \cdot \boldsymbol{V}$$

$$\mathbf{P} = \begin{bmatrix} \mathbf{Z}_1^{-1} & & & 0 \\ & \mathbf{Z}_2^{-1} & & \\ & & \ddots & \\ 0 & & & \mathbf{Z}_N^{-1} \end{bmatrix}$$

D. M. Solís, V. F. Martín, M. G. Araújo, D. Larios, F. Obelleiro, and J. M. Taboada, “Accurate EMC Engineering on Realistic Platforms Using an Integral Equation Domain Decomposition Approach,” ***IEEE Trans. Antennas Propag.***, vol. 68, no.4, pp. 3002 – 3015, Apr. 2020,

Solving a multiscale radiation problem

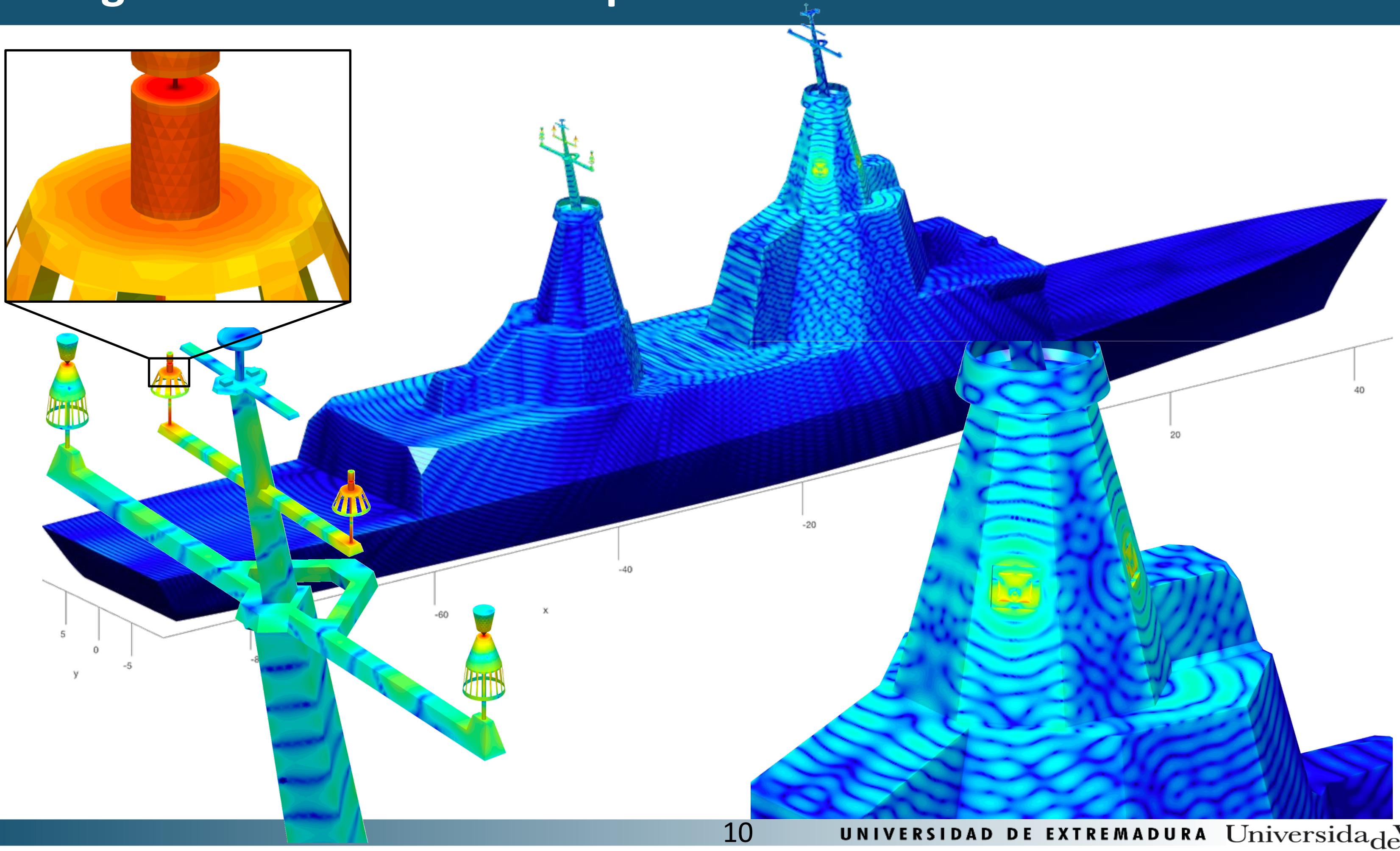

Solving a multiscale radiation problem. Speeding-up convergence.

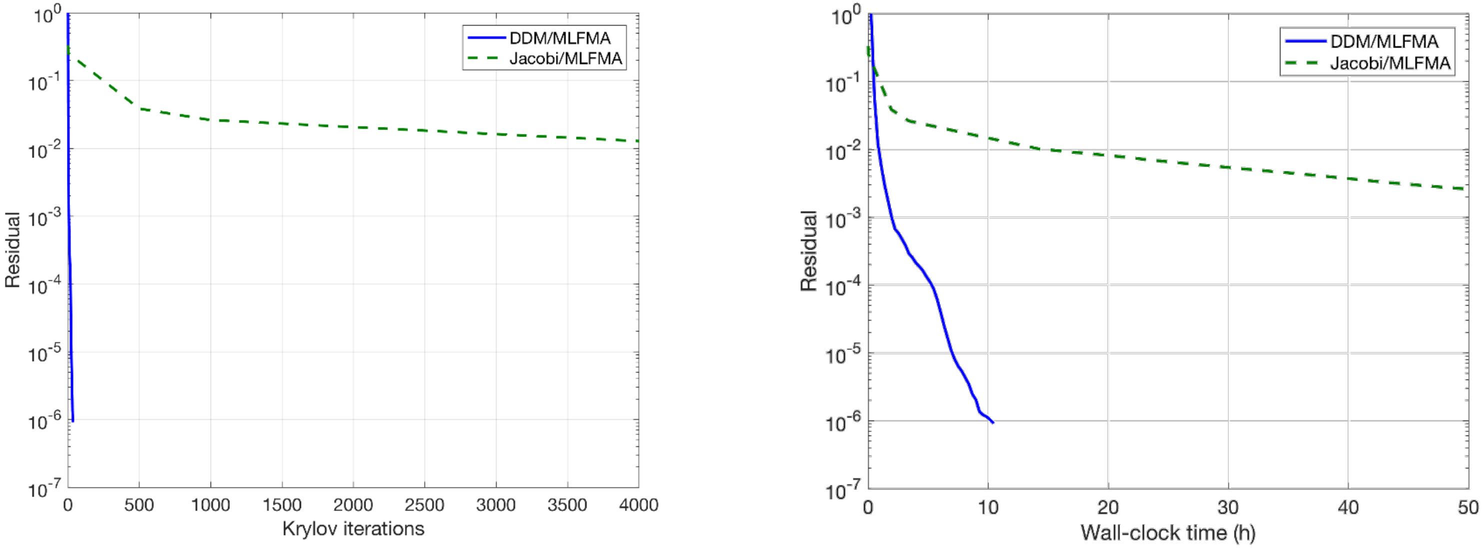

- 4 Intel Xeon E7-8867v3 microprocessors, with a total of 64 cores (no hyperthreading) and 1 TB RAM.
- Residual error up to 10^{-6} in 10 hours
- DDM is not parallelized, but the MLFMA-FFT solver of the local sub-domains
- The **speed-up is only due to the improvement of convergence posed by DDM**, not due to the DDM parallel propensity.

Discontinuous Galerking (DG)

- We apply DG to the collection of surfaces composing the entire problem.
- Nonconformal meses are allowed across the tear lines and junctions between different surfaces.

Half-RWG

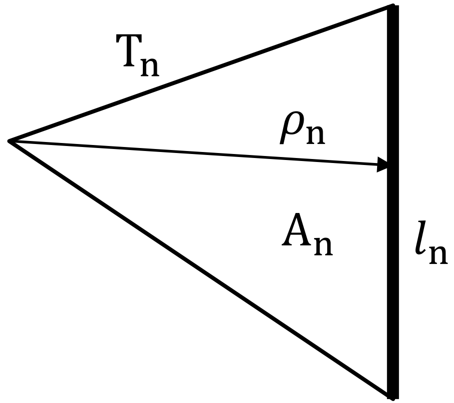

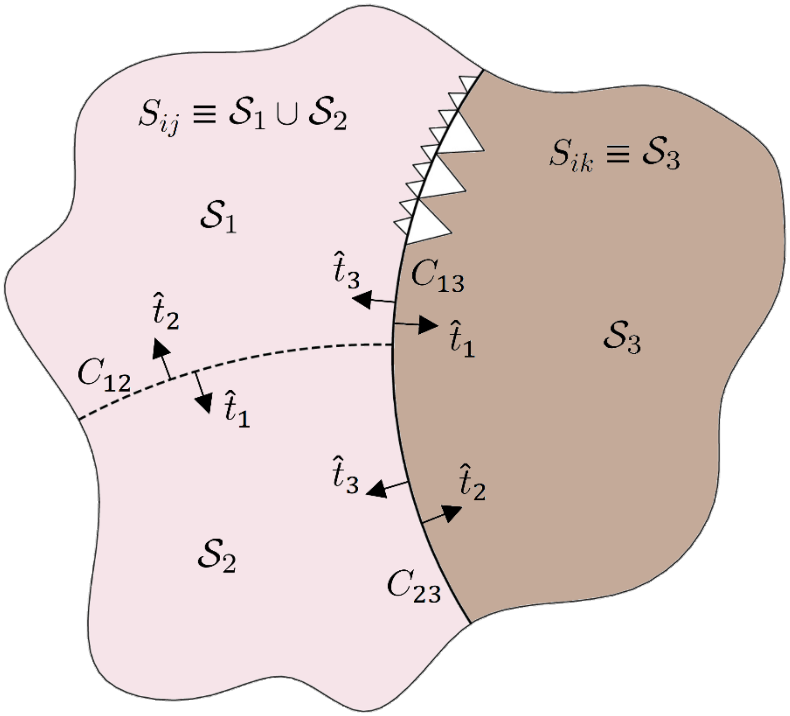

Discontinuous Galerking (DG)

- Product rule for divergence
- Divergence Gauss theorem
- half-RWG normal component does not vanish at the boundary contour (non-div-conforming basis/testing function)

$$\mathcal{L}_i(\mathbf{X}_i) = jk_i \int_S \mathbf{X}_i(\mathbf{r}')g_i(\mathbf{r},\mathbf{r}')dS' + \frac{1}{jk_i}\nabla \int \mathbf{X}_i(\mathbf{r}')\nabla' g_i(\mathbf{r},\mathbf{r}')dS'$$

h-RWG terms

$$\begin{aligned} A^i_{mn} = \int_{\Delta_m} \mathbf{f}_m \cdot \mathcal{L}_i(\mathbf{f}_n)dS = &\int_{\Delta_m} \mathbf{f}_m \int_{\Delta_n} \mathbf{f}_n g_i(\mathbf{r},\mathbf{r}')dS'dS && \text{(SSI)}\\ &-\frac{1}{jk_i}\Big[\int_{\Delta_m} \nabla\cdot\mathbf{f}_m \int_{\Delta_n} \nabla'\cdot\mathbf{f}_n g_i(\mathbf{r},\mathbf{r}')dS'dS && \text{(SSI)}\\ &-\int_{\Delta_m} \nabla\cdot\mathbf{f}_m \oint_{\partial S_n} \hat{m}_n\cdot\mathbf{f}_n g_i(\mathbf{r},\mathbf{r}')d\partial S'dS && \text{(SLI)}\\ &-\oint_{\partial S_m} \hat{m}_m\cdot\mathbf{f}_m \int_{\Delta_{n|i}} \nabla'\cdot\mathbf{f}_n g_i(\mathbf{r},\mathbf{r}')dS'd\partial S && \text{(LSI)}\\ &+\oint_{\partial S_m} \hat{m}_m\cdot\mathbf{f}_m \oint_{\partial S_n} \hat{m}_n\cdot\mathbf{f}_n g_i(\mathbf{r},\mathbf{r}')d\partial S'd\partial S\Big] && \text{(LLI)} \end{aligned}$$

$$\begin{aligned} A'^i_{mn} = \int_{\Delta_m} \mathbf{f}_m \cdot \hat{n}_m \times \mathcal{L}_i(\mathbf{f}_n)dS = &\int_{\Delta_m} (\mathbf{f}_m\times\hat{n}_m) \int_{\Delta_n} \mathbf{f}_n g_i(\mathbf{r},\mathbf{r}')dS'dS && \text{(SSI)}\\ &-\frac{1}{jk_i}\Big[\int_{\Delta_m} \nabla\cdot(\mathbf{f}_m\times\hat{n}_m) \int_{\Delta_n} \nabla'\cdot\mathbf{f}_n g_i(\mathbf{r},\mathbf{r}')dS'dS && \text{(SSI)}\\ &-\int_{\Delta_m} \nabla\cdot(\mathbf{f}_m\times\hat{n}_m) \oint_{\partial S_n} \hat{m}_n\cdot\mathbf{f}_n g_i(\mathbf{r},\mathbf{r}')d\partial S'dS && \text{(SLI)}\\ &-\oint_{\partial S_m} \hat{m}_m\cdot(\mathbf{f}_m\times\hat{n}_m) \int_{\Delta_n} \nabla'\cdot\mathbf{f}_n g_i(\mathbf{r},\mathbf{r}')dS'd\partial S && \text{(LSI)}\\ &+\oint_{\partial S_m} \hat{m}_m\cdot(\mathbf{f}_m\times\hat{n}_m) \oint_{\partial S_n} \hat{m}_n\cdot\mathbf{f}_n g_i(\mathbf{r},\mathbf{r}')d\partial S'd\partial S\Big] && \text{(LLI)} \end{aligned}$$

[1] V. F. Martín, L. Landesa, F. Obelleiro, and J. M. Taboada, "A Discontinuous Galerkin Combined Field Integral Equation Formulation for Electromagnetic Modeling of Piecewise Homogeneous Objects of Arbitrary Shape," ***IEEE Trans. Antennas Propag.***, vol 70, no 1, pp. 487 - 498 Jan. 2022

Interior Penalty (IP)

$$\oint_{\partial S_m} \hat{m}_m \cdot \mathbf{f}_m \oint_{\partial S_n} \hat{m}_n \cdot \mathbf{f}_n g_i(\mathbf{r},\mathbf{r}') d\partial S' d\partial S$$ → Result Unbounded!

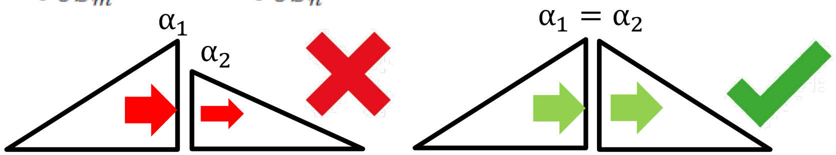

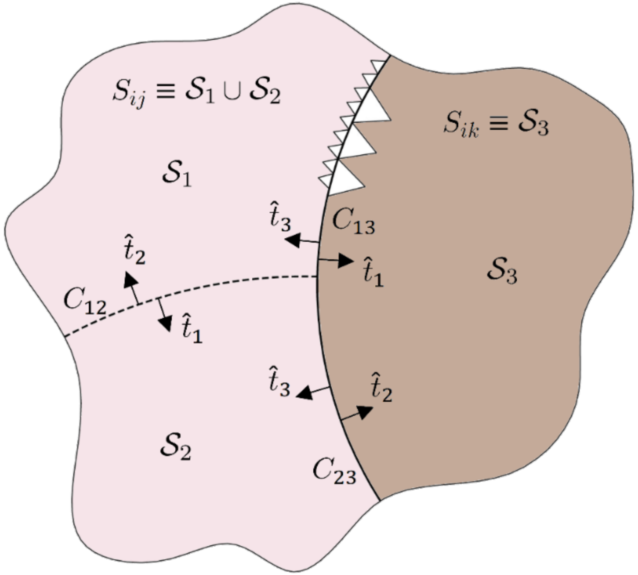

IP term: normal current continuity

$$\hat{t}_k \cdot \mathbf{X}_k + \hat{t}_{k'} \cdot \mathbf{X}_{k'} = 0 \quad \text{on} \quad C_{kk'}$$

$$\sum_{\substack{\partial S_m \\ \in C_k}} \sum_{\substack{\partial S_n \\ \in C_{k'}}} (\hat{m}_m \cdot \mathbf{f}_m X_m + \hat{m}_n \cdot \mathbf{f}_n X_n) = 0 \quad \text{on} \quad C_{kk'}$$

$$\frac{\beta}{jk_i} \sum_{\substack{\partial S_m \\ \in C_k}} \int_{\partial S_m} \hat{m}_m \cdot \mathbf{f}_m \sum_{\substack{\partial S_n \\ \in C_{k'}}} (\hat{m}_m \cdot \mathbf{f}_m X_m + \hat{m}_n \cdot \mathbf{f}_n X_n) \, d\partial S = 0 \quad \text{on} \quad C_{kk'}$$

$$IP_{mn}^{i} = \frac{\beta}{jk_i} \int_{\partial S_m} \hat{m}_m \cdot \mathbf{f}_m \, \hat{m}_n \cdot \mathbf{f}_n \, d\partial S$$

[1] V. F. Martín, L. Landesa, F. Obelleiro, and J. M. Taboada, "A Discontinuous Galerkin Combined Field Integral Equation Formulation for Electromagnetic Modeling of Piecewise Homogeneous Objects of Arbitrary Shape," *IEEE Trans. Antennas Propag.*, vol 70, no 1, pp. 487 - 498 Jan. 2022

Plasmonic Au nanocubes with Ag depositions over dielectric substrate

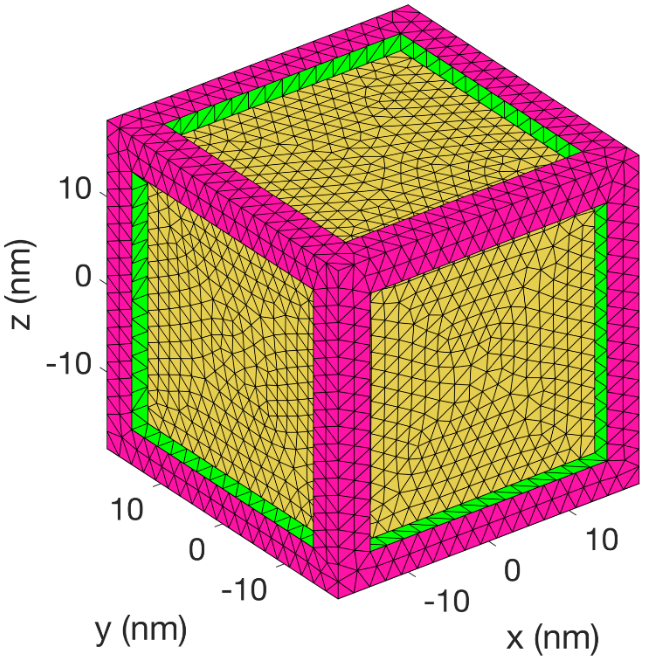

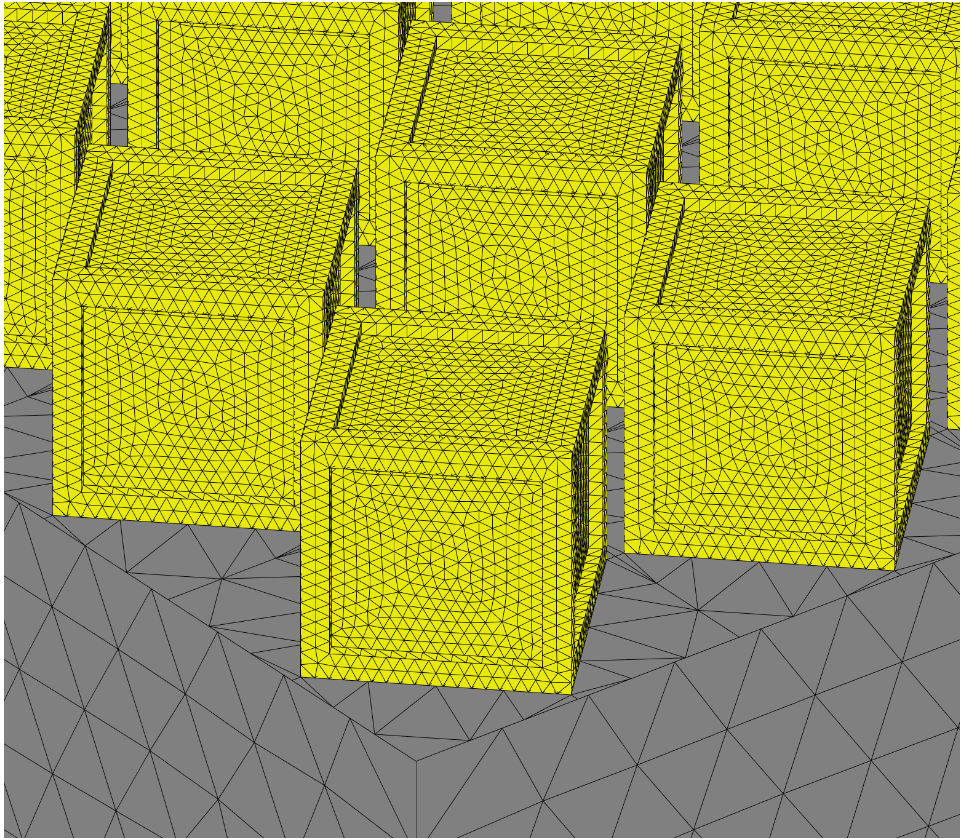

Plasmonic Au nanocubes with Ag depositions over dielectric substrate

- Equivalent electric currents induced on the external boundary surfaces.

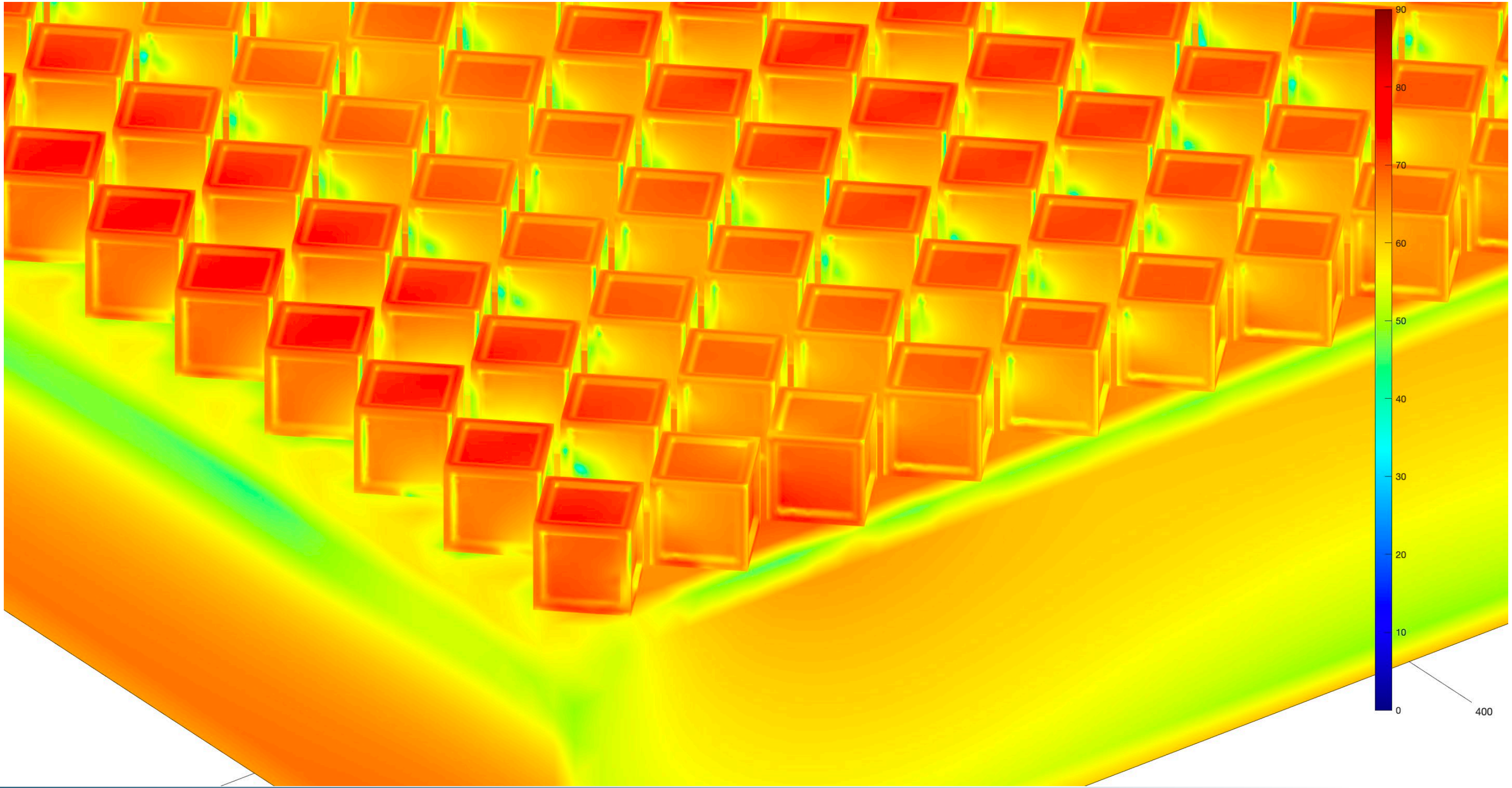

Convergence

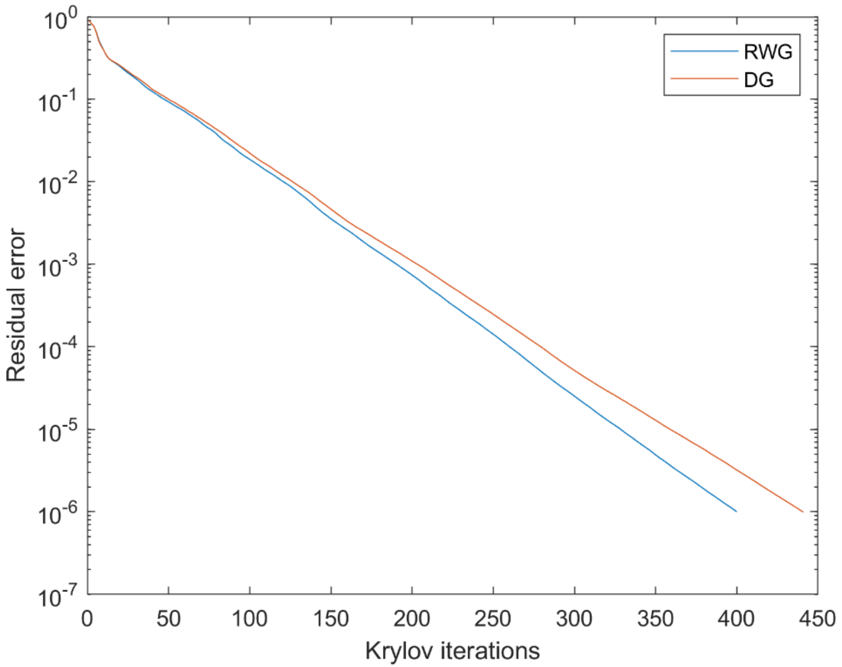

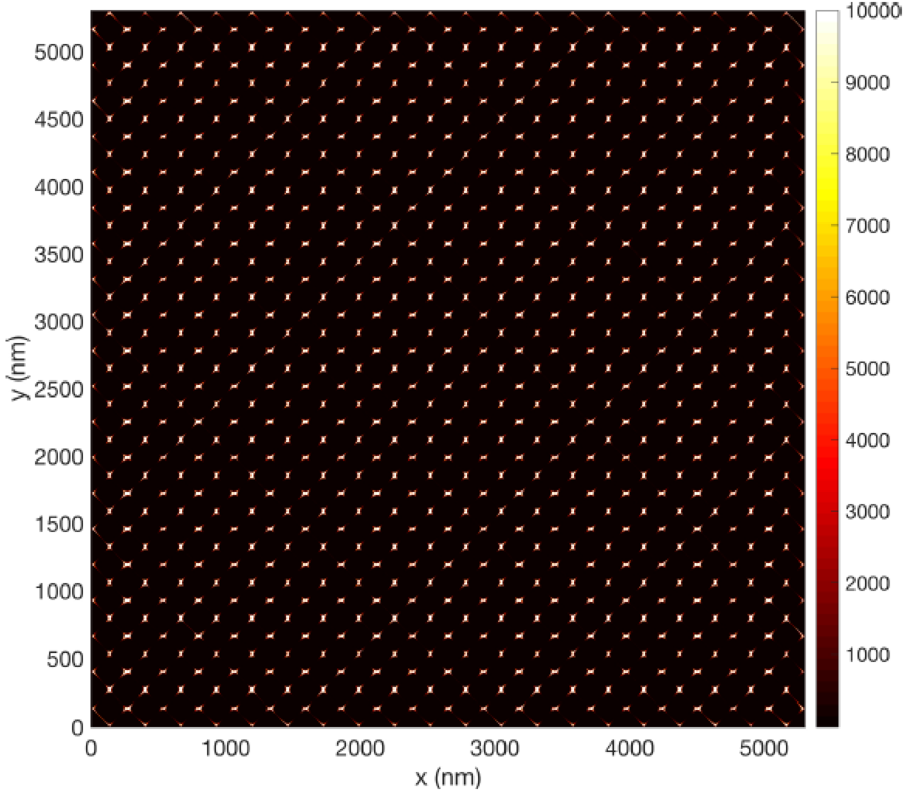

Multiresolution (MR) Preconditioner

1. Generalized basis functions.

- Reproduce behavior of input RWG.
- Lineal combination of RWG or gRWG.
- $\mathbf{f}_i^l(\boldsymbol{r}) = \sum_{n=1}^{N_i^{l-1}} f_{i,n}^l \, \mathbf{f}_{\mu_i^l(n)}^{l-1}(\boldsymbol{r})$
- $\nabla \cdot$ operator $[Q_i^l][f_i^l] = [q_i^l]$
- And the generalized coefficients are obtained

$$\begin{bmatrix} [\hat{Q}_i^l] \\ [U_i^l] \end{bmatrix} [f_i^l] = \begin{bmatrix} [\hat{q}_i^l] \\ [0] \end{bmatrix}$$

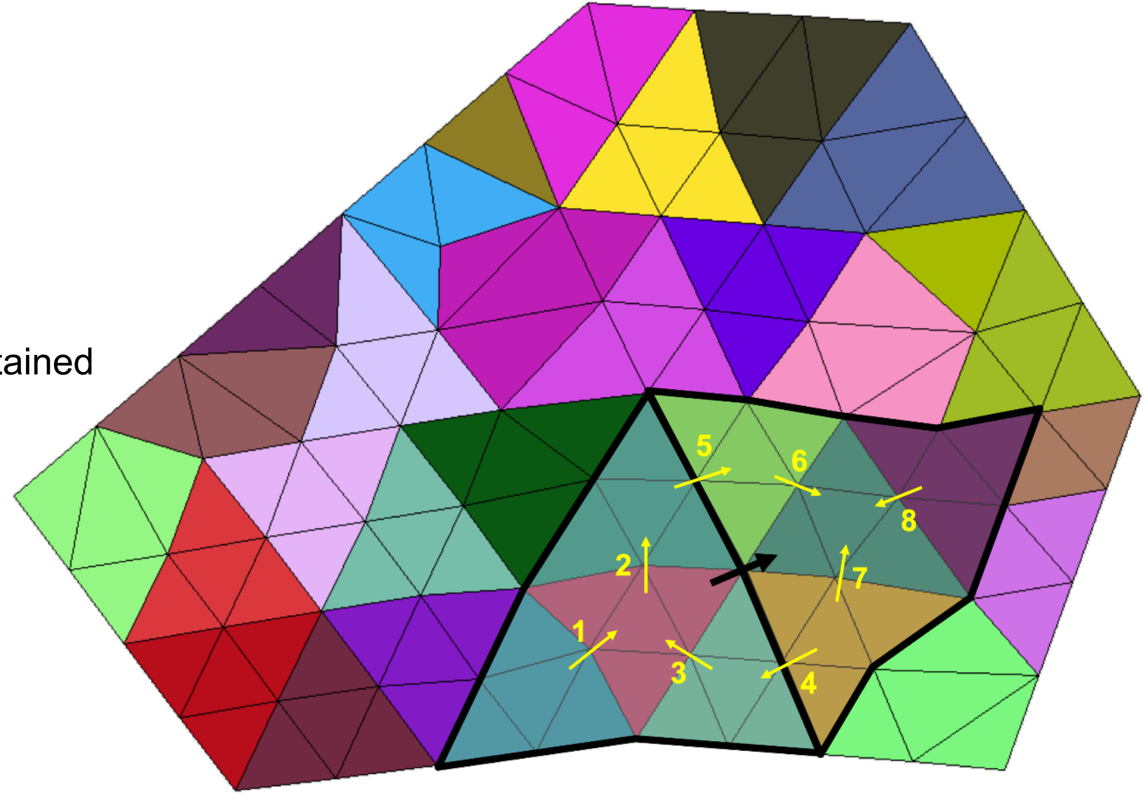

[1] V. F. Martin, J. M. Taboada and F. Vipiana, "A Multi-Resolution Preconditioner for Non-Conformal Meshes in the MoM Solution of Large Multi-Scale Structures," in *IEEE Transactions on Antennas and Propagation*, 2023

Multiresolution (MR) Preconditioner

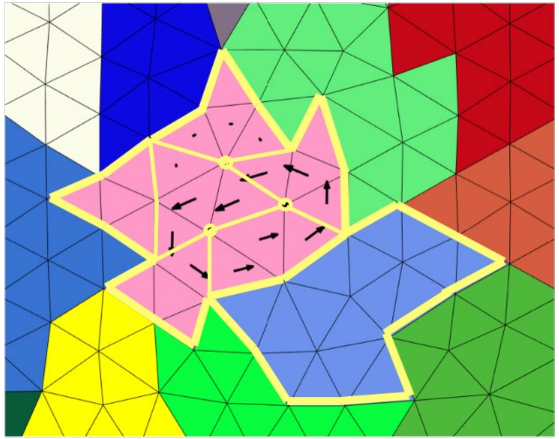

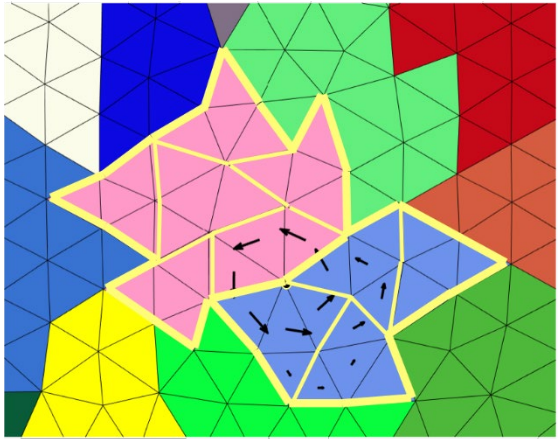

3. Multiresolution basis functions.

- Non-solenoidal.
- Solenoidal (1).
- Solenoidal (2).

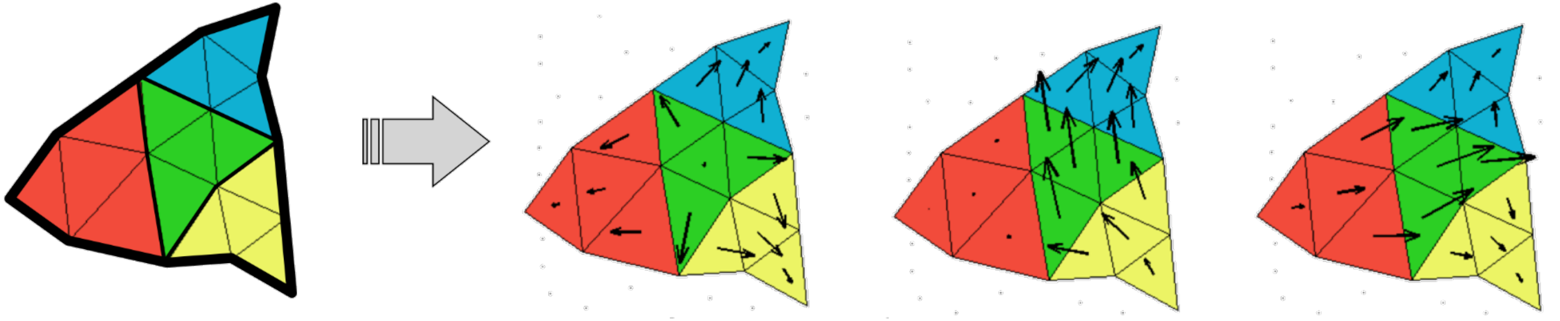

[1] V. F. Martin, J. M. Taboada and F. Vipiana, "A Multi-Resolution Preconditioner for Non-Conformal Meshes in the MoM Solution of Large Multi-Scale Structures," in ***IEEE Transactions on Antennas and Propagation***, 2023

DDM + MR

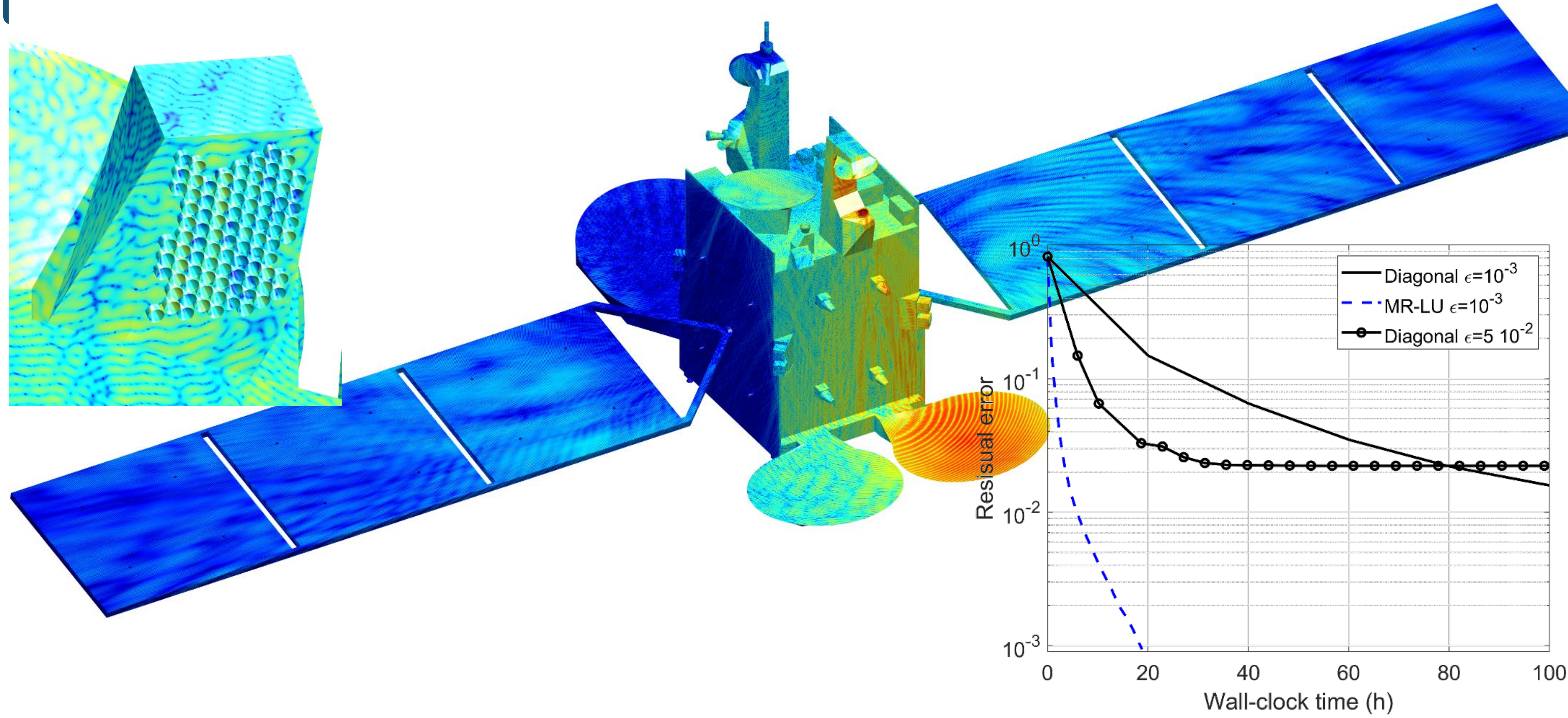

[1] V. F. Martin, J. M. Taboada and F. Vipiana, "A Multi-Resolution Preconditioner for Non-Conformal Meshes in the MoM Solution of Large Multi-Scale Structures," in ***IEEE Transactions on Antennas and Propagation***, 2023

RCS

RCS@10 GHz
Fuselage
Nose radome
Nose radar

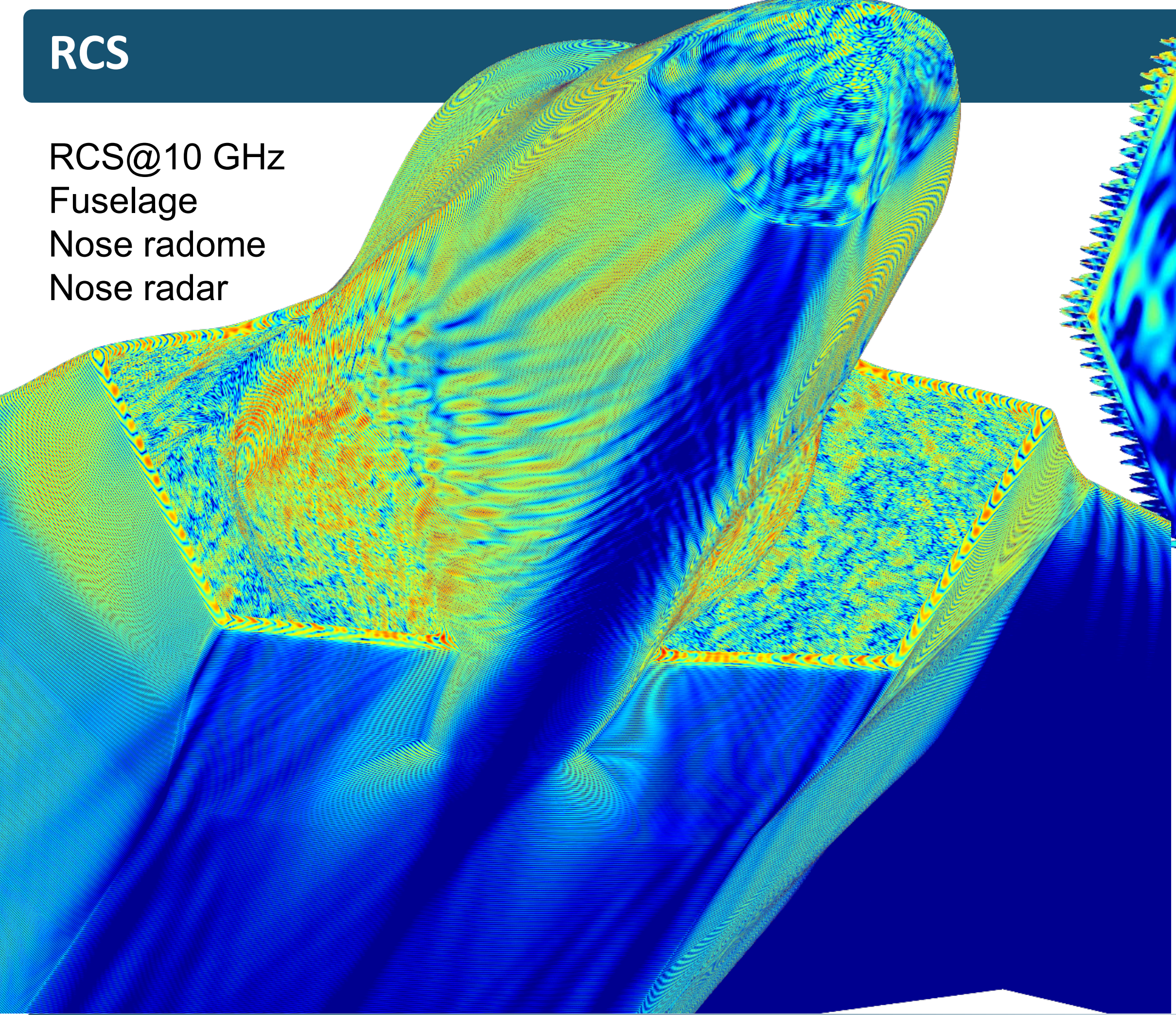

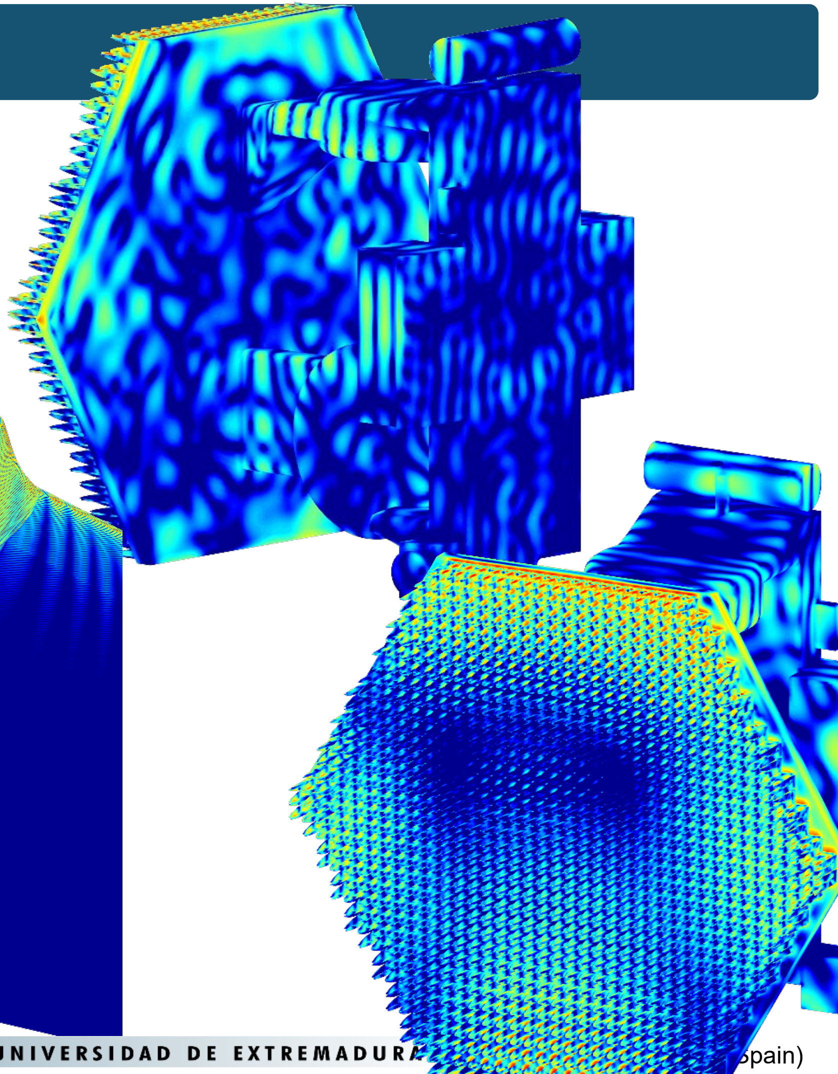

RCS

RCS@10 GHz
Fuselage
Nose radome
Nose radar

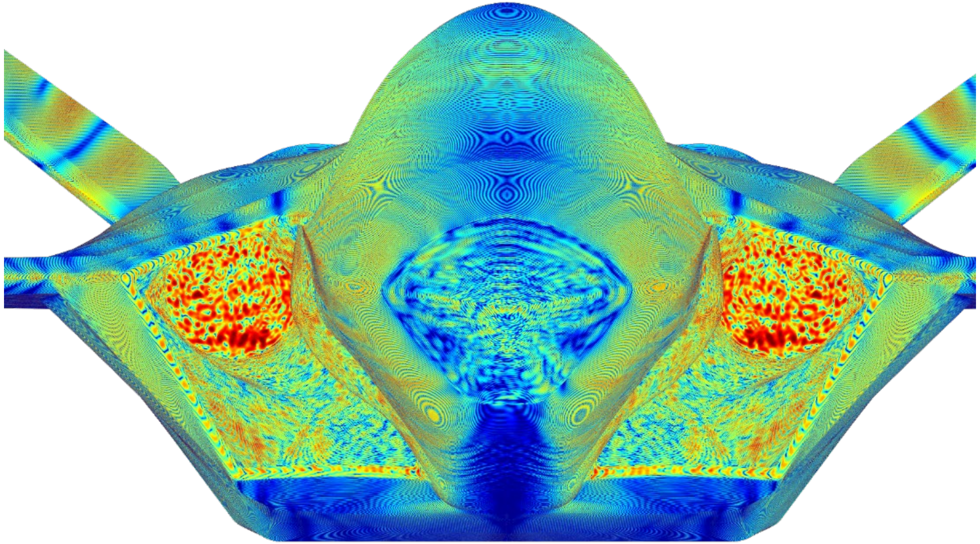

Plasmonic systems for optical biosensors

- Surface enhanced Raman spectroscopy (SERS): single-molecule detection
- Inelastic (non-linear) Raman scattering: Laser interaction with the molecular vibrational modes → energy shift to blue and red (Raman shift)
- Raman spectrum is like a molecule fingerprint
- Plasmonic substrates can enhance the Raman scattering (SERS) by factors up to 10^{10}

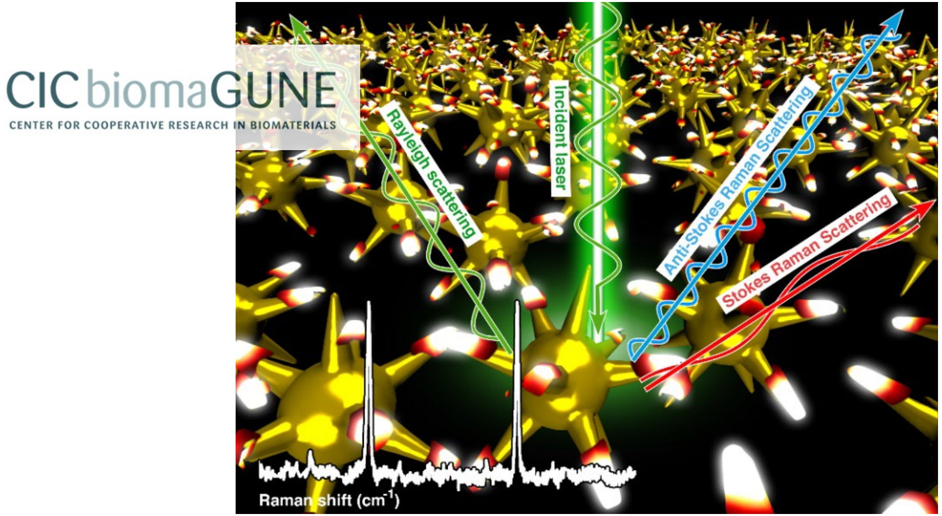

$$\Delta\omega(cm^{-1}) = \left(\frac{1}{\lambda_0(nm)} - \frac{1}{\lambda_1(nm)}\right) 10^7 \frac{(nm)}{(cm)}$$

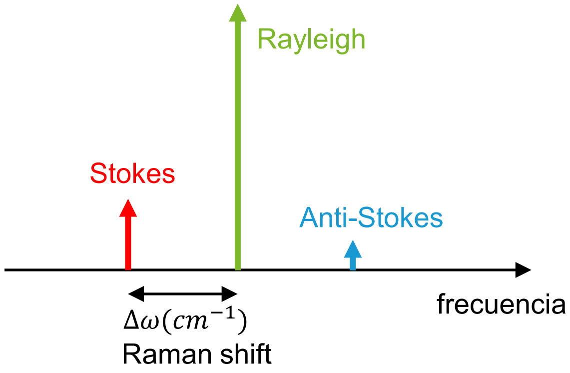

[1] D. M. Solís, J. M. Taboada, F. Obelleiro, L. M. Liz-Marzán, and F. J. García de Abajo, "Toward ultimate nanoplasmonics modeling", ***ACS Nano***, vol. 8, no. 8, pp. 7559-7570, August 2014.

Chryral nanocrystals

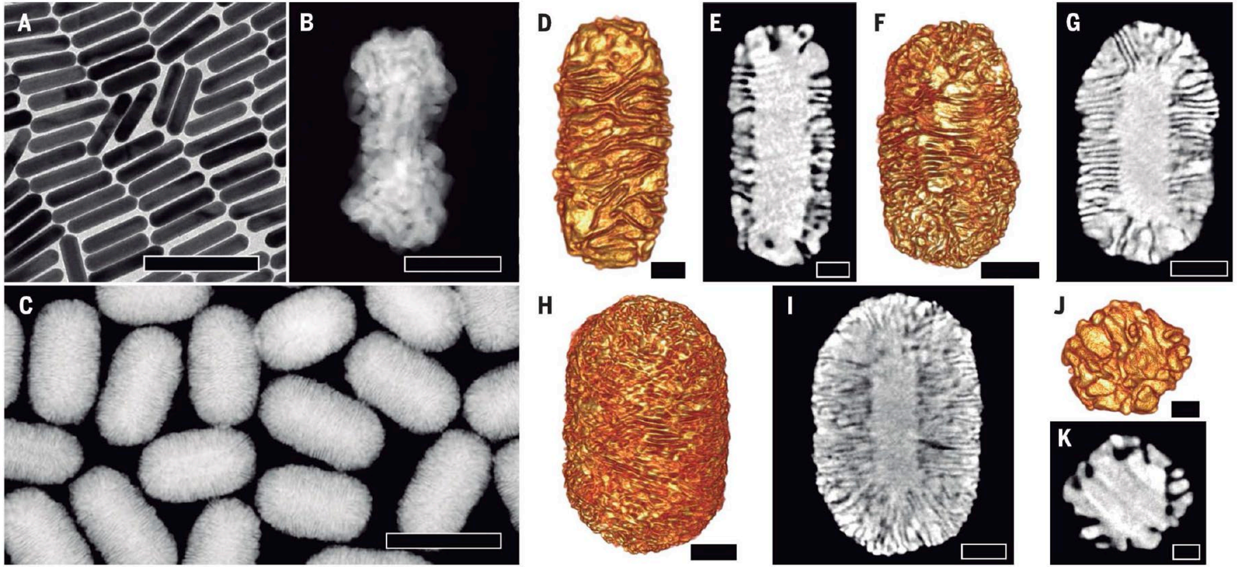

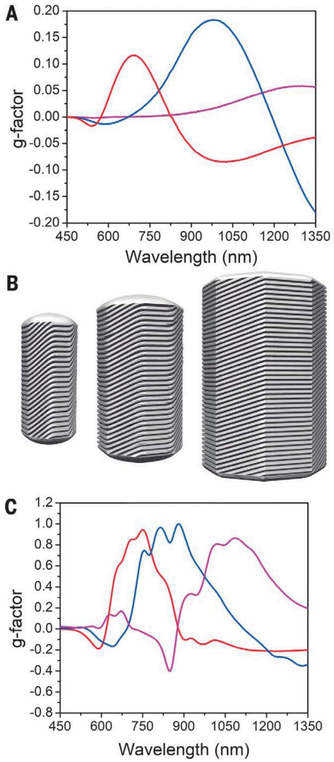

G. González-Rubio, J. Mosquera, V. Kumar, A. Pedrazo-Tardajos, P. Llombart, D. M. Solís, I. Lobato, E. G. Noya, A. Guerrero-Martínez, J. M. Taboada, F. Obelleiro, L. G. MacDowell, S. Bals, L. M. Liz-Marzán, "Micelle-directed chiral seeded-growth on anisotropic gold nanocrystals," ***Science***, vol. 368, no. 6498, pp. 1472-1477, June 2020.

DNA pogrammed superlattices

Northwestern | IIN INTERNATIONAL INSTITUTE FOR NANOTECHNOLOGY

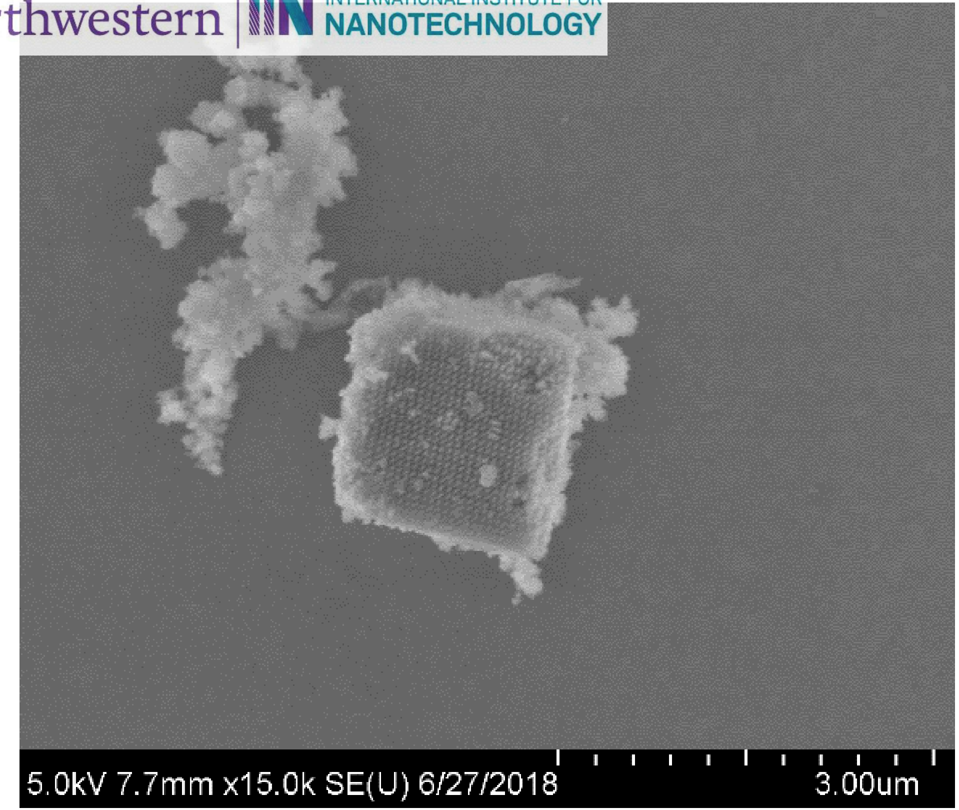

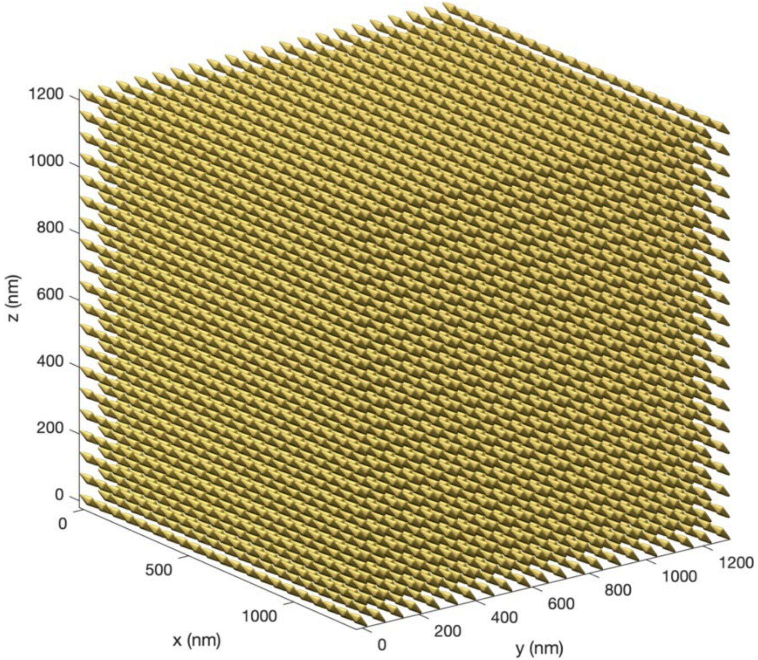

Under review in ***Science***

Anisotropic optical response: birefringence

Northwestern | IIN INTERNATIONAL INSTITUTE FOR NANOTECHNOLOGY

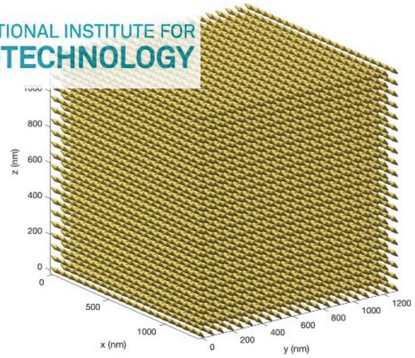

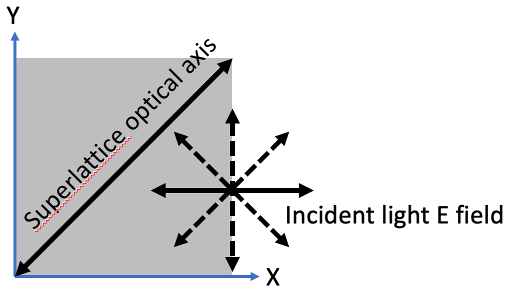

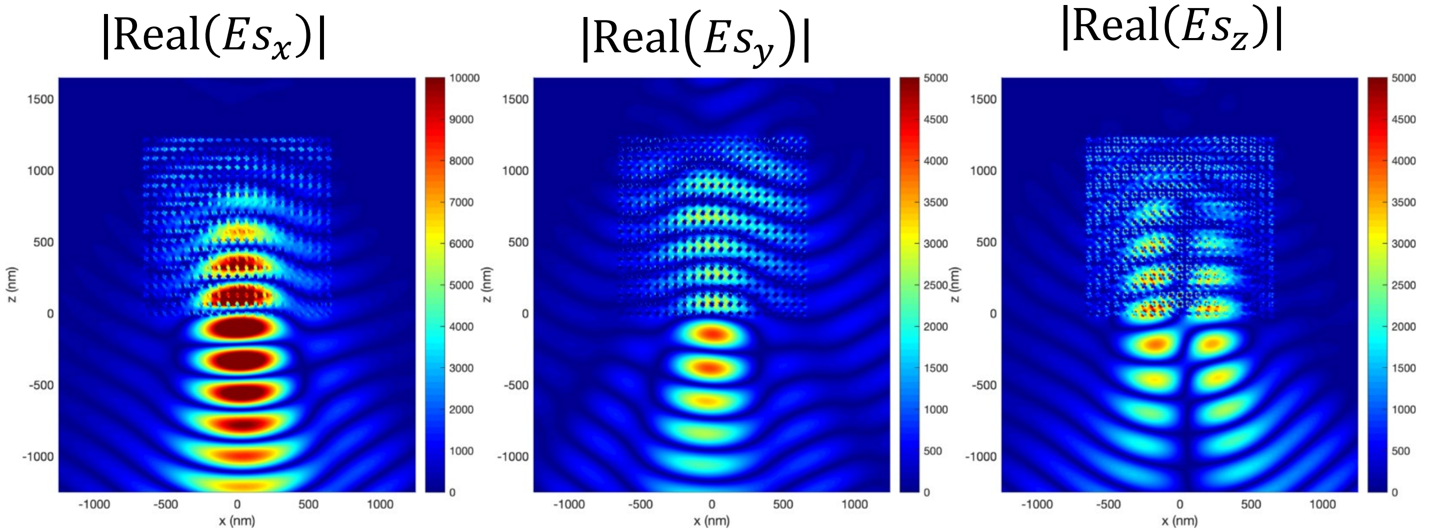

UNIVERSIDAD DE EXTREMADURA Universidade Vigo (Spai

Anisotropic optical response: birefringence

Northwestern | INTERNATIONAL INSTITUTE FOR NANOTECHNOLOGY

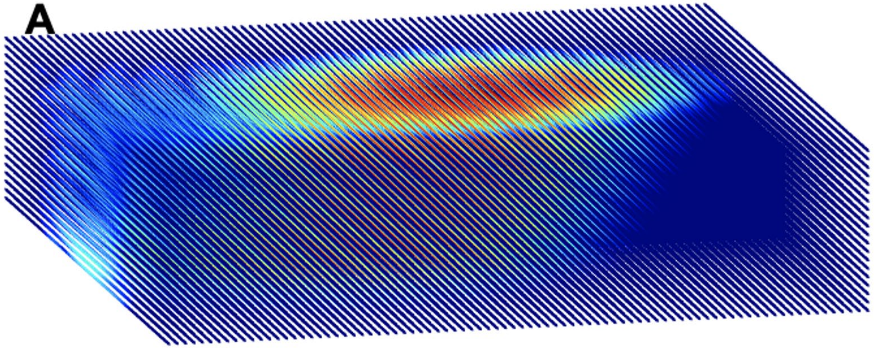

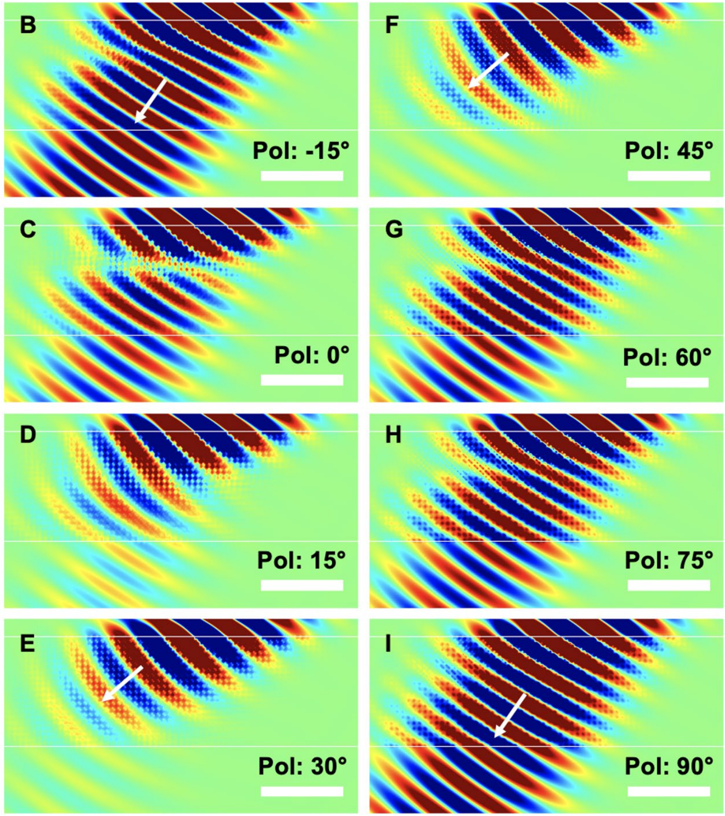

Acknowledgment

This work was supported in part by the Spanish Ministerio de Ciencia, Innovación y Universidades under Project PID2020-116627RB-C21, Project PID2020-116627RB-C22, funded by MCIN/ AEI/10.13039/501100011033 and grant FPU00550/17, and the Extremadura local government and European Union FEDER (GR18055, IB18073).

MINISTERIO DE CIENCIA E INNOVACIÓN

AGENCIA ESTATAL DE INVESTIGACIÓN

Unión Europea

Fondo Europeo de Desarrollo Regional

Una manera de hacer Europa

JUNTA DE EXTREMADURA

Consejería de Economía, Ciencia y Agenda Digital

Anisotropic optical response: birefringence

Northwestern | INTERNATIONAL INSTITUTE FOR NANOTECHNOLOGY

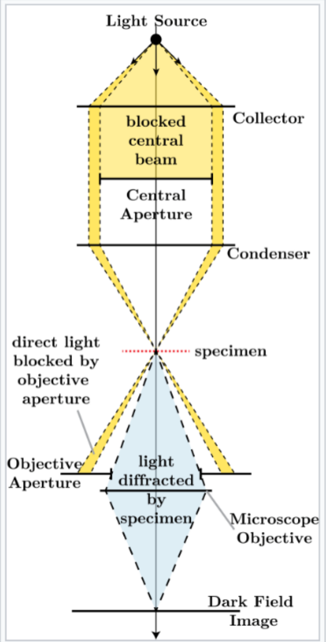

Diagram illustrating the light path through a dark-field microscope

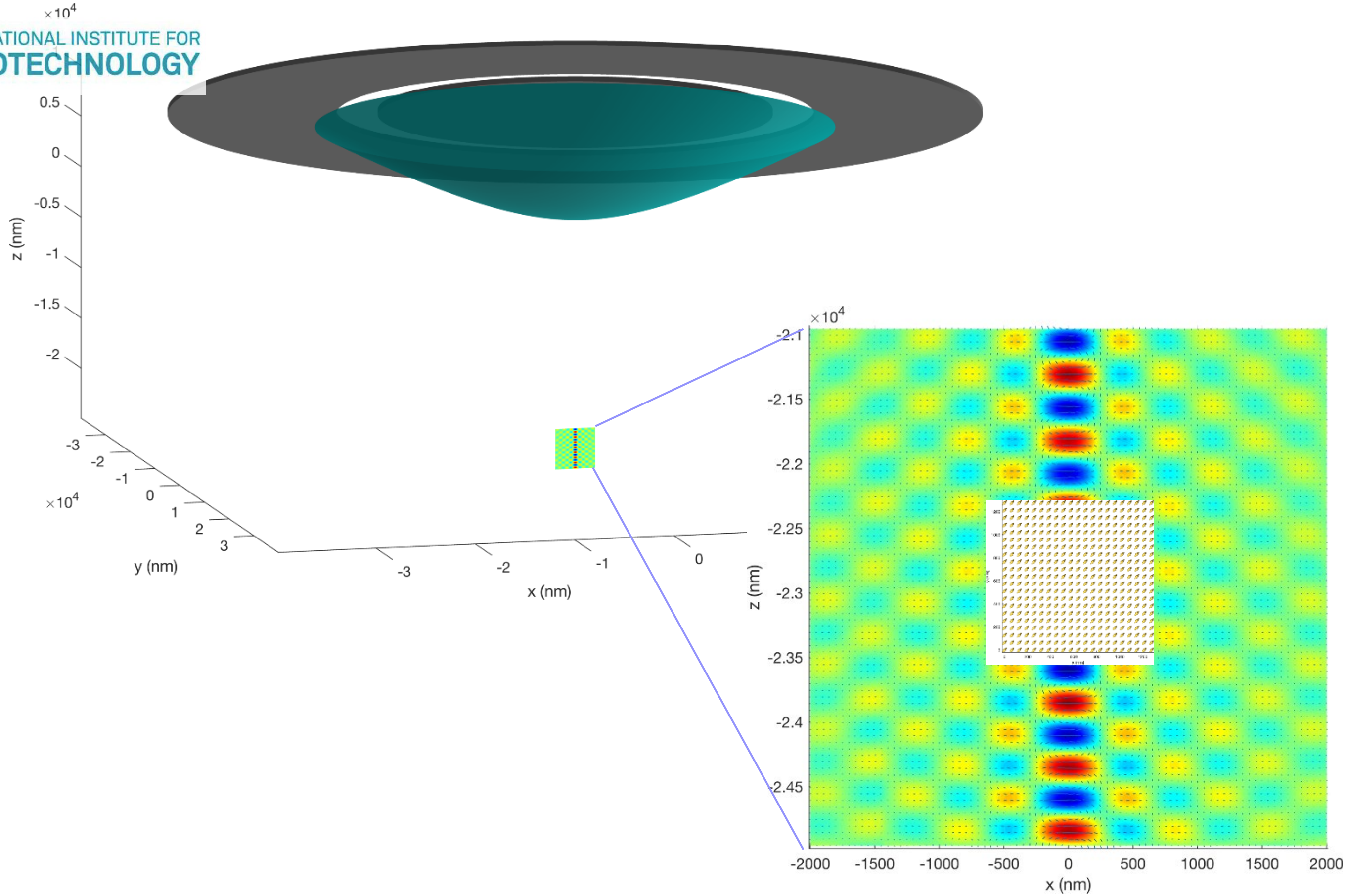

UNIVERSIDAD DE EXTREMADURA Universidade Vigo (Spai